



ISSN: 0976-3376

Available Online at <http://www.journalajst.com>

ASIAN JOURNAL OF  
SCIENCE AND TECHNOLOGY

Asian Journal of Science and Technology  
Vol. 08, Issue, 06, pp.4902-4911, June, 2017

## RESEARCH ARTICLE

### CHANNEL PLANFORM MIGRATION ARCHITECTURE OF MEANDERING RIVERS

<sup>1,2</sup>Zhipeng Lin, <sup>1,2</sup>Le Chen, <sup>1,2</sup>Jingfu Shan and <sup>3</sup>Qianjun Sun

<sup>1</sup>Key Laboratory of Exploration Technologies for Oil and Gas Resources, Ministry of Education, Yangtze University, Wuhan 430100, China;

<sup>2</sup>School of Geosciences, Yangtze University, Wuhan 430100, China;

<sup>3</sup>School of Energy Resources, China University of Geosciences, Beijing 100083, China

#### ARTICLE INFO

##### Article History:

Received 17<sup>th</sup> March, 2017

Received in revised form

26<sup>th</sup> April, 2017

Accepted 04<sup>th</sup> May, 2017

Published online 30<sup>th</sup> June, 2017

##### Key words:

Meandering river;  
Planform migration architecture;  
Migration patterns;  
Architecture elements;  
Satellite images.

#### ABSTRACT

The planform migration architecture is the basis for the reconstruction and restoration of the sedimentary evolution of the paleochannel, as well as the premise for forecasting the migration trend of the river. This paper aims to figure out the regularity of the planform migration structures of a meandering river, and historical satellite images are acquired primarily through Google Earth and ACME Mapper. Through the characterization on Irtysh River, which is relatively in the considerable preservation condition of the natural structure, 28 kinds of structure elements are utilized to depict the meandering river. Moreover, 5 kinds of characterization factors are proposed to make quantitative describe the channel structure, extraordinarily, three of which are firstly brought forward and applied here. Via the fine anatomy of the structure of 12 typical meander loops, S, C,  $\Delta\theta$ ,  $\Delta\theta'$ ,  $K_M$  factors are adopted to summarize 6 kinds of planform migration structures. Finally, 9 meandering channel migration patterns are concluded.

Copyright©2017, Zhipeng Lin et al., This is an open access article distributed under the Creative Commons Attribution License, which permits unrestricted use, distribution, and reproduction in any medium, provided the original work is properly cited.

#### INTRODUCTION

Reconstruction of meandering sedimentary and evolution process needs to understand the planform migration architecture, at this stage, the basic theoretical research is relatively insufficient. The cognition for the migration regular pattern of the meandering channel is the key to dissecting the sedimentary structure of the ancient river (Blum et al., 2013; Schuurman et al., 2016; Kasvi et al., 2017; Lin et al., 2017). What's more, the internal structure of the river sand body is complex, and the traditional method is difficult to accurately characterize the internal architecture of the reservoir unit and predict the hydrocarbon-derived model of oil and gas production process (Xue 1991; Wu and Wang 1999; Mu 2000; Yin et al., 2001; Hu 2016; Hu et al., 2017). By characterizing and analyzing the law of channel planform migration architecture of meandering rivers, it will be easier to guide and understand the distribution characteristics of underground sand bodies in underground space (Sui 2006; Willis and Tang 2010; Mithun et al., 2012; Hu et al., 2017). It is one of the most

important methods to summarize the process of planform migration architecture for fluvial, especially meandering river. Although an increasing amount of literature focus on the ancient and modern fluvial sedimentary system, the process evolution analysis on the dynamic geomorphology of meanders remains a challenge (Willis and Tang 2010; Ielpi and Ghinassi 2014; Debnath et al., 2017). Many classical articles at home and abroad try to analyze the three-dimensional dynamic structure of the river from the aspects of scale estimation, numerical simulation, and hydrodynamics, such as Leopold and Maddock (1953), had made some achievements on river hydrodynamic characteristics, meandering structure, pattern (1957) and geomorphological features (1960) and so on. Wolman and Miller (1960) thought that the periodicity of flow change is an important factor in controlling the geomorphology through the analysis of the geomorphic process, and followed the examples of tracking the evolution of the meandering process. Williams (1978) proposed the definition and calculation of bank-full discharge by analyzing the river bank flow and speculated its influence on the channel morphology. Brice (1974) put forward four main categories of meander loops, including simple symmetrical, simple asymmetrical, compound symmetrical, and compound asymmetrical. Researches of the fluvial system from Miall (1985; Miall 2013; Miall 2014; Miall 2016),

\*Corresponding author: <sup>1,2</sup>Le Chen

<sup>1</sup>Key Laboratory of Exploration Technologies for Oil and Gas Resources, Ministry of Education, Yangtze University, Wuhan 430100, China;

<sup>2</sup>School of Geosciences, Yangtze University, Wuhan 430100, China;

indicated that the best clues were always determined on the considerable visible field outcrops, which could be understood from the configuration elements to the evolution of sedimentology, deepening the finding of the historical process. Therefore, The structural and evolutionary levels of migration architecture of meandering rivers need to be further strengthened. The morphological evolution, especially the meandering channel, considerably plays a certain role in controlling the lithology and reservoir physical properties. The changes of the translation, rotation, and expansion of meanders will surely cause the transform of the channel shape, thus influencing the underground reservoir architectures (Hooke 1980; Hooke 1984; Gilvear *et al.*, 2000). In recent years, domestic and foreign researchers have begun to carry on the dynamic geomorphology analysis of planform migration evolution structure of meandering rivers. Significant results such as Ghinassi *et al.*, (2014); Ielpi and Ghinassi (2014), through the analysis of the architectural and dynamic geomorphology of the meandering river in northern Scarborough, Yorkshire, United Kingdom, combined with the planform and vertical sections of outcrops of extensive three-dimensional exposures, a comprehensive model of facies distribution was developed.

Wu *et al.*,(2015; 2016) analyzed the evolution of river sediments by reconstructing the migration pattern of composite point bars of outcrop and examining ancient exhumed channel belts, eventually established a semi-quantitative channel migration model; Ghinassi *et al.*,(2014; 2016) focused on the planform evolution and stratal architecture of the meandering channel and discussed it as an important method to reconstruct the palaeoflow and facies distribution and develop the fluvial hydrocarbon reservoirs. Schuurman *et al.*,(2016) observed the morphological changes and migration of meandering river by establishing morphological numerical model experiments. Thus it can be seen this topic that it is necessary to understand the process of the evolution of the planform migration architecture of meandering river. This paper aims to explore the planform migration architecture of meandering rivers and the basic rule and pattern. By means of high-resolution historical satellite images from Google Earth and ACME Mapper (A kind of software based on Google Earth), the research characterizes on Irtysh River, which is relatively in the considerable preservation condition of the natural architecture and free from the impact of human beings. For these targets, we will try to characteristic the morphological elements of planform architecture of meandering rivers and

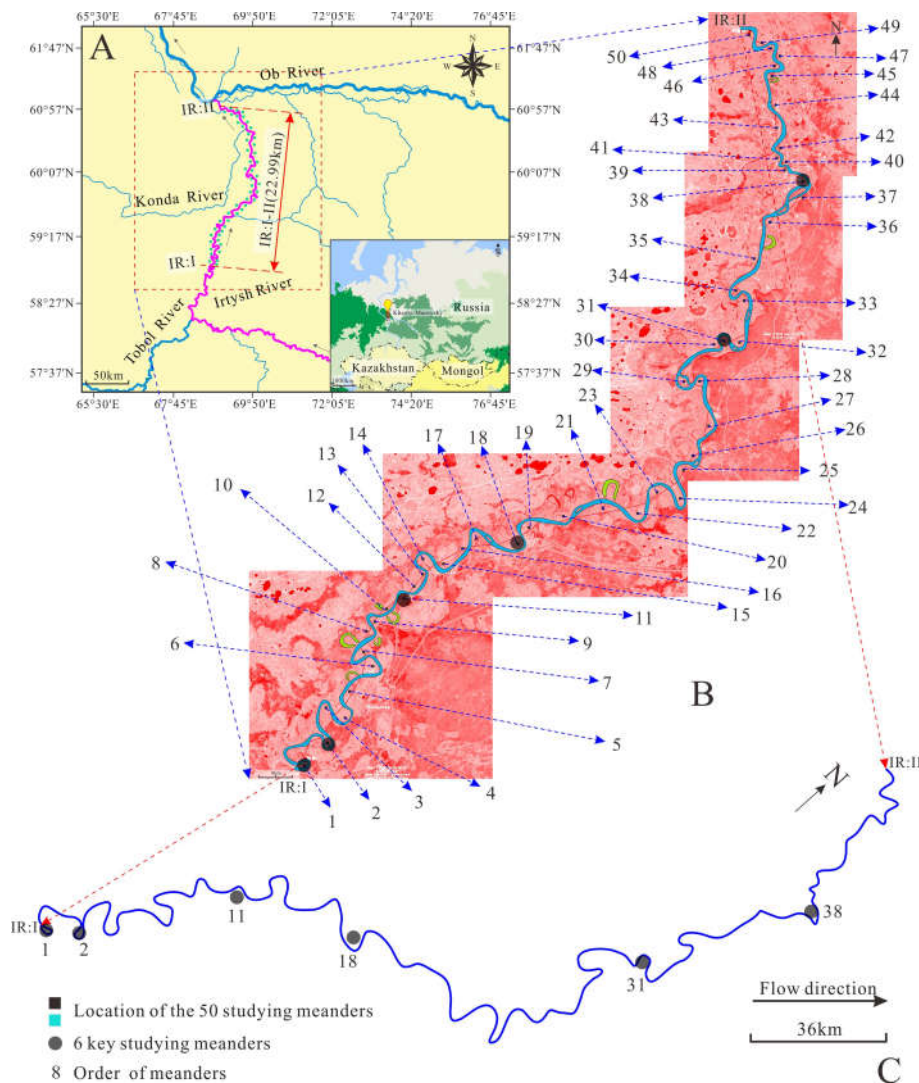


Figure 1. Location map of the Irtysh River: A 50 meanders are investigated in reach IR: I-II, coordinate information comes from Google Earth and ACME Mapper. B the details of the 50 studying meanders in the composite satellite images of Google Earth, showing the orders of the meanders. C extracted centerline(see Figure 2) from the research drainage area of the Irtysh River, marked the 6 key studying meanders

understand the geomorphology process and migration characteristics of different meandering channels.

**Geology Background**

The research here chooses the Irtysh River. Within this river, 50 meanders are selected for investigation and 6 of them are utilized for comprehensive characterizing. The Irtysh River is one of the largest tributaries of the Ob River, which is about 4248 km long and flows from the southeast to the northwest of the Altai Mountains, Xinjiang, China, flows via Kazakhstan North into Russia, in the Khanty-Mansyky importing into the Ob River. The study area lies from the north of Tobolsk, with coordinates of 60°56'N and 69°19'E, as shown in Figure 1, for reach IR: I-II, with a length of 44.51 km and a straight line distance of 22.99 km. The meandering structure is preserved relatively in good condition and easier to observe.

**Terminology and Elements**

The planform architecture of a meandering river is the basis for depicting the channel migration process. Although the morphology characteristics of a large number of meandering rivers on the modern alluvial plain have been identified, the description and characterization of the meandering river in the field of sedimentology are still mainly in the interpretation of sedimentary microfacies (He and Wang 2008; Zhu 2008; Feng 2013). Methods that combined with geomorphology are few, so here we overall and systematically improve the terminology and elements of planform architecture of meandering river. Furthermore, based on the analysis of the structure of the meandering rivers in the study of sedimentology and geomorphology at home and abroad (Brice 1974; Willis and Tang 2010; Mithun, Dabojani *et al.*, 2012; Wu, Ullah *et al.*, 2016; Fryirs 2017; Kasvi, Laamanen *et al.*, 2017), we propose

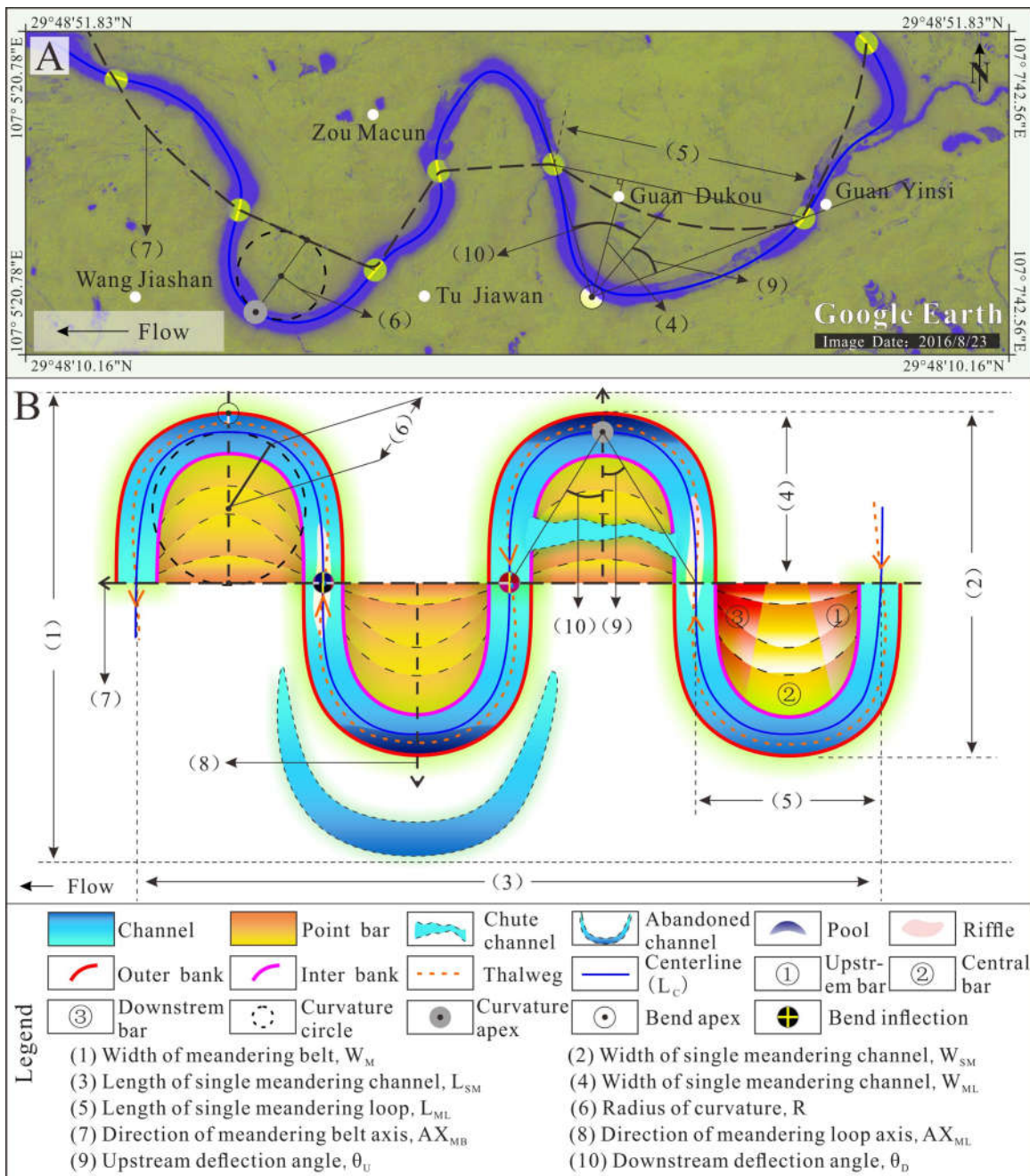


Figure 2. Planform elements of migration architecture of the meandering river: A satellite images of Longxi River in Chongqing, China, taken on August 23, 2016, from Google Earth, the direction of the water flow is from right to left, the shape is easy to express structural elements. B the idealized meandering migration architecture model, which includes 17 static elements and 12 dynamic elements

a new set of characterization elements for meandering migration architecture, extraordinarily, three of the parameters are firstly brought forward and applied in this paper. Overall, the elements can be divided into 3 parts: static elements, dynamic elements, and characterization parameters.

**Static elements**

The static elements refer to the geomorphic deposition unit and the abstract concept streamline which can be adopted to describe qualitatively the plane structure of the meandering river. It mainly includes the in-channel elements: main channel, pool, riffle, thalweg, centerline, bend inflection, and curvature apex. And the outbank elements are: meandering belt, point bar (upstream bar, central bar, downstream bar), chute channel, outer bank (concave bank), the inner bank (convex bank), meandering loop (meander or bend), abandoned channel, floodplain(overbank), curvature circle, and bend apex. Among them, the major elements for plane migration structure characterization are the following ones like a meandering loop, centerline, bend inflection, curvature apex, curvature circle, point bar, and thalweg.

**Dynamic elements**

The dynamic elements refer to the quantitative parameter extracted from the static elements, which is the quantitative reflection and presentation of the channel structure. The numerical change can indicate the migration architecture of the meandering river to a certain extent. It mainly include scalar element and vector element, the former includes: width of meandering belt ( $W_M$ ), length of meandering belt ( $L_M$ ), width of single meandering channel ( $W_{SM}$ ), length of single meandering channel ( $L_{SM}$ ), width of single meandering loop ( $W_{ML}$ ), length of single meandering loop ( $L_{ML}$ ), length of channel centerline( $L_C$ ), and radius of curvature( $R$ ). While the latter includes: meandering belt axis ( $AX_{MB}$ ), meandering loop axis ( $AX_{ML}$ ), upstream deflection angle ( $\theta_U$ ), and downstream deflection angle ( $\theta_D$ ), (Table 1, Figure 2).

**Characterization parameters**

The static and dynamic elements are representative of the characteristics of the channel structure, however, in order to quantify the characteristics of the migration architecture, structural elements for the dynamic evolution of meandering process need to do feature analysis, that is, characterization parameters. According to the structural elements above, five characterization parameters are extracted: sinuosity index (S), curvature (C), difference of along-current deflection angle ( $\Delta\theta$ ), difference of counter-current deflection angle ( $\Delta\theta'$ ), and expansion coefficient ( $K_M$ ), in which the parameters of  $\Delta\theta$ ,  $\Delta\theta'$  and  $K_M$  are presented with a tentative for the first time in this paper while the parameters of S and C is also demonstrated with a new idea. The basic elements and characterization parameters of the river segment are shown in Table 1. Sinuosity index (S) refers to the ratio of the length of centerline to the corresponding meandering belt axis, which is adopted to indicate the bending degree. The definition of the sinuosity previously is the ratio of the length of the channel to the valley. However, evidently, the problem is that how to understand the definition of the length channel, valley, outer bank line, interbank line, thalweg, and centerline, or the length of the straight line of the starting and ending points of the

river. The distinction is not clear enough that the characterization of sinuosity is likely to cause confusion. Nevertheless, with this new definition, using the length of the centerline to represent the length of a river, the confusion of channel length can get unified. Simultaneously, the utilization of the length of meandering belt axis instead of length of valley, on the one hand, will not cause the fuzzy of concept; On the one hand, as mentioned earlier, the length of meandering belt axis rather than the straight distance from the beginning to the end point could accurately reflect the sinuosity situation, since it takes into account the migration of channel morphology with the terrain meandering factors, rather than simplifying the distance as a straight line. Expressed as a formula can be written:

$$S = L_C / |AX_{MB}| \dots\dots\dots (1)$$

Curvature (C) refers to the reciprocal of curvature radius (R) of corresponding research meander, which is taken to indicate the degree and scale of a meander. The greater the curvature is, the greater the degree of the channel bending is. The method of calculating curvature according to the ratio between the arc length and the diameter of a point bar(Shi *et al.*, 2012) has a certain degree of ambiguity because the extracted diameter and the arc length from the irregularity of the point bar are not clear for lack of accurate definition. Here the choice of R is of great concern, which is not a simple half of the so called diameter of a point bar. Firstly, through the two bend inflections one can determine the starting and end point of the meander. Secondly, define the curvature apex and control the shape of the entire meandering loop. Ultimately, through these three points: two bend inflections and one curvature apex, the thus obtained curvature circle and R could be an effectively better representative for the truth of curvature. Expressed as the formula below:

$$C = 1 / R \dots\dots\dots (2)$$

The difference of along-current deflection angle ( $\Delta\theta$ ) refers to the difference between the upstream deflection angle ( $\theta_U$ ) and downstream deflection angle ( $\theta_D$ ), reflecting the symmetry of a bend. The closer the value is to 0, the higher the symmetry of the meandering loop is. Moreover, while the value is positive and greater, the curvature apex is indicated closer to the upstream bend inflection, showing a tendency of counter-current rotation. On the contrary, the difference is negative and smaller, the curvature apex is indicated closer the downstream bend inflection, showing a tendency of along-current rotation. Formula is:

$$\Delta\theta = \theta_U - \theta_D \dots\dots\dots (3)$$

Meanwhile, contrary to  $\Delta\theta$ , the  $\Delta\theta'$ , difference of counter-current deflection angle, refers to the difference between the downstream deflection angle ( $\theta_D$ ) and upstream deflection angle ( $\theta_U$ ), with objective similarity and perspective diversity. The closer the value is to 0, the higher the symmetry of the meandering loop is. While the value is positive and greater, the curvature apex is indicated closer to the downstream bend inflection, showing a tendency of along-current rotation. On

the contrary, the difference is negative and smaller, the curvature apex is indicated closer the upstream bend inflection, showing a tendency of counter-current rotation. Write as

$$\Delta\theta' = \theta_D - \theta_C \dots\dots\dots (4)$$

Expansion coefficient ( $K_M$ ) refers to the ratio of the length of single meandering loop ( $L_{ML}$ ) to the diameter of curvature circle ( $2R$ ). Basically this coefficient could represent the changes of meandering shape because it is dominated by the elements of both bend reflection and curvature apex. When the meandering loop migrates outward with expansion, the curvature diameter ( $2R$ ) tends to be generally larger with the control of bend reflection, while the length of single meandering loop relatively changes less. Thus the value of  $K_M$  decreases gradually to 1. When the meander expands to a certain extent, constriction process begins. Within the course, the curvature diameter is generally going to be larger than the length of the single meandering loop, leading to the value of  $K_M$  decreases to less than 1. This is the course of how the  $K_M$  could quantitatively reflect the situation of expansion and constriction process of a channel. See as a formula:

$$K_M = L_{ML} / 2R \dots\dots\dots (5)$$

next turn of lateral erosion and accumulation process, so the whole migration architecture of a channel is always showing the trend of outward expansion with repeated paces, which is the overall principle. According to the variation trend of streamline from beginning to end of the migration process and combined with quantitative characterization with the elements and parameters, the planform migration architecture can be divided into two categories: expansion and constriction structure (Figure 3 and 4).

**Expansion Structure**

The Expansion Structure (ES) is featured as the constant outward migration process of the channel, and  $K_M$  is usually greater than 1. According to the swing difference of meandering loops and point bar and the value of  $\Delta\theta$  and  $\Delta\theta'$ , it can be specifically subdivided into 3 parts (Figure 3): Symmetrical Expansion Structure, Upstream Rotation Expansion Structure, and Downstream Rotation Expansion Structure.

**Symmetrical Expansion Structure**

The meandering loop continuously erodes the outer banks and the symmetry is good,  $K_M$  is greater than 1 and  $\Delta\theta$  is close to

**Table 1. The Planform Architecture Elements and Parameters of the 6 Key Studying Meanders in the reach IR: I-II**

Elements	Irtysch River					
	1	2	11	18	31	38
Meander						
Latitude	58°52'N	58°56' N	59°20' N	59°34' N	60°14' N	60°40' N
Longitude	68°47'E	68°50'E	68°52'E	69°17'E	69°48'E	69°52'E
$W_M/m$	16520.9	14479.6	13068.9	14855.1	10522.0	22592.7
$L_M/m$	302741	302741	302741	302741	302741	302741
$W_{SM}/m$	12263.0	9765.0	2467.3	12230.8	7394.3	13075.5
$L_{SM}/m$	11094.8	11813.2	8409.4	23525.6	17068.8	18441.5
$W_{ML}/m$	3821.3	2541.6	1758.1	3225.5	2642.6	3309.8
$L_{ML}/m$	919.7	2472.9	3551.9	7637.9	2282.7	3145.0
$L_C/m$	10166.9	7305.9	4626.3	11994.3	6999.2	6315.5
$R/m$	2155.3	1389.6	729.7	2148.5	1318.1	1311.9
$ AX_{MB} /m$	919.7	2472.8	3551.9	7637.9	2282.7	3145.0
$AX_{MB}/^\circ$	344.3	103.7	211.8	226.9	49.7	336.5
$AX_{ML}/^\circ$	44.0	136.9	311.9	94.4	316.8	110.1
$\theta_U/^\circ$	9	20	50	18	30	34
$\theta_D/^\circ$	12	13	55	55	28	15
S	11.05	2.95	1.30	1.57	3.07	2.01
C	0.0005	0.0007	0.0014	0.0005	0.0008	0.0008
$\Delta\theta/^\circ$	-3	7	-5	-37	2	19
$\Delta\theta'/^\circ$	3	-7	5	37	-2	-19
$K_M$	0.22	0.89	2.43	1.78	0.87	1.20

Note:  $W_M$ : width of meandering belt,  $L_M$ : length of meandering belt,  $W_{SM}$ : width of single meandering channel,  $L_{SM}$ : length of single meandering channel,  $W_{ML}$ : width of single meandering loop,  $L_{ML}$ : length of single meandering loop,  $L_C$ : length of channel centerline,  $R$ : radius of curvature,  $|AX_{MB}|$ : length of meandering belt axis,  $AX_{MB}$ : direction of meandering belt axis,  $AX_{ML}$ : direction of meandering loop axis,  $\theta_U$ : upstream deflection angle,  $\theta_D$ : downstream deflection angle, S: sinuosity index, C: curvature,  $\Delta\theta$ : difference of along-current deflection angle,  $\Delta\theta'$ : difference of counter-current deflection angle,  $K_M$ : expansion coefficient.

**Planform migration structure of meandering channels**

The existing researches for the channels are mainly qualitative descriptions of the shape and direction of the point bar, but lack of quantification. In this paper, our point is to conduct quantitative study of the meandering channel with the characterization parameters. At the same time, analyze and explore the planform migration architecture of meandering rivers. The role of the river on the bank is always expressed as the erosion of the outer bank and accumulation of the inner bank, as time went by, loops could get cut off when the bend laterally shifts to a certain extent. Followed by repeating the

$0^\circ$ , this is the Symmetrical Expansion Structure (SES). As shown in Figure 3 IR1-IR3, IR1 shows the satellite images of meander 11 from years 1984 to 2014, the migration of bend 11 is not obvious. Through the planform migration architecture of IR2 and characterization parameters of IR3, we can see that the value of S is 1.3, C is 0.0014, reflecting that the bending degree is in general;  $\Delta\theta$  is  $-5^\circ$  and  $\Delta\theta'$  is  $5^\circ$ , indicating that the symmetry of the meander is relatively better with a slight trend of along-current rotation.  $K_M$  is 2.43, indicating that the river is in the expansion period, and the degree of expansion is small. Comprehensively, the meander 11 shows the architecture of SES.

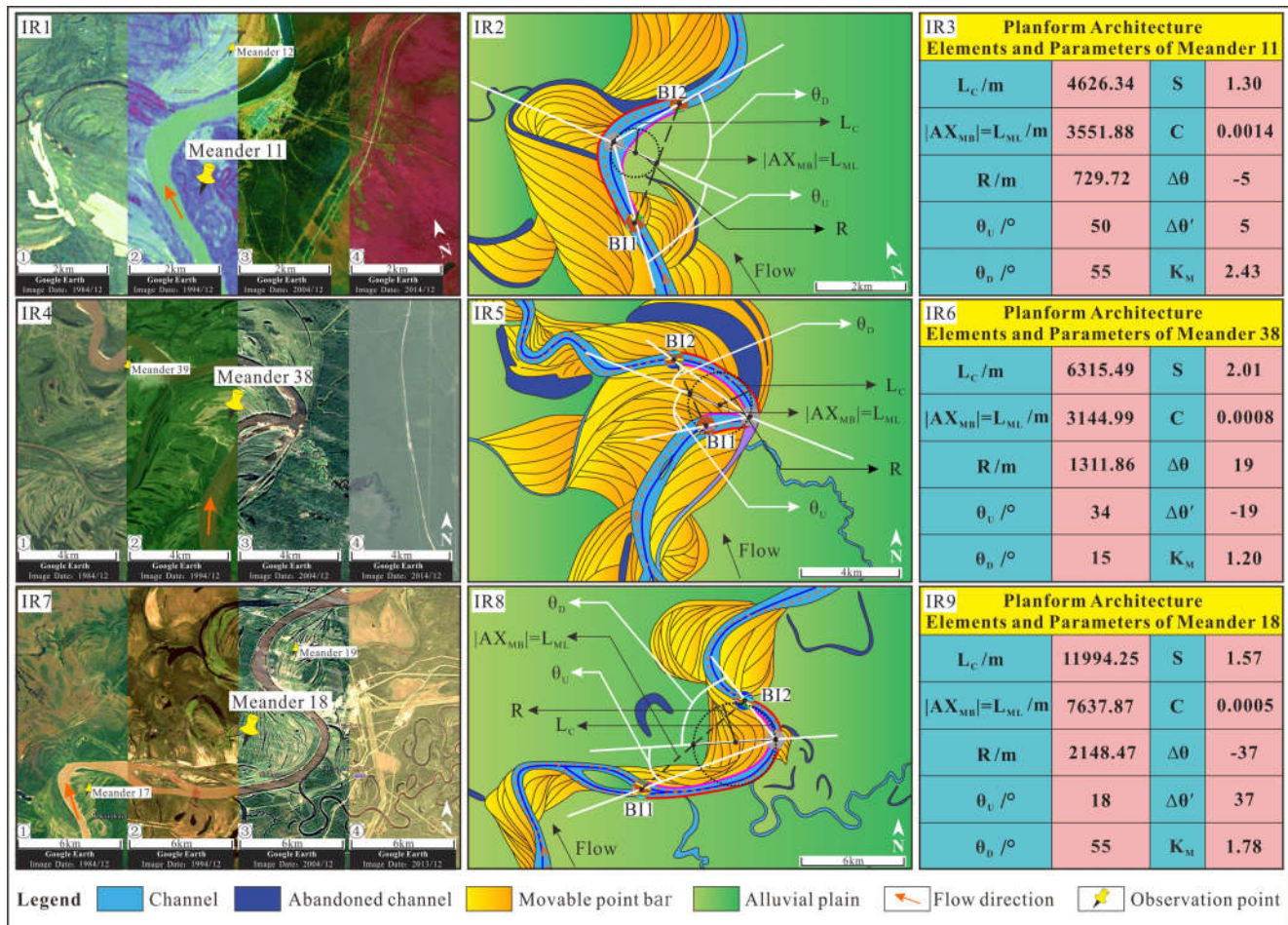


**Figure 3. Planform migration architecture of the Expansion Structure of the Irtys River:** IR1-IR3 is the performance of Symmetrical Expansion Structure in meander 11, while IR1 shows the satellite images taken in the last 30 years and coordinates are 59°20'N and 68°52'E; IR2 shows the planform migration architecture in details, and IR3 shows the statistical data of planform migration architecture elements and parameters of meander 11. IR4-IR6 is the performance of Upstream Rotation Expansion Structure in meander 38, while IR4 shows the satellite images taken in the last 30 years and coordinates are 60°40'N, 69°52'E; IR5 shows the planform migration architecture in details, and IR7 shows the statistical data of planform migration architecture elements and parameters of meander 38. IR7-IR9 is the performance of Downstream Rotation Expansion Structure in meander 18, while IR7 shows the satellite images taken in the last 30 years and coordinates are 64°45'N, 154°20'E; IR8 shows the planform migration architecture in details, and IR9 shows the statistical data of planform migration architecture elements and parameters of meander 18. Images and coordinates information come from Google Earth and ACME Mapper

### Upstream Rotation Expansion Structure

The meandering loop continuously erodes the outer banks with curvature apex being closer to the upstream bend inflection, showing a tendency of counter-current rotation,  $K_M$  is greater than 1 and  $\Delta\theta$  is positive, this is the Upstream Rotation Expansion Structure (URES). As shown in Figure 3 IR4-IR6, IR4 shows that from years 1984 to 2014, the migration of the meander 38 in the Irtys River is weak. Through the planform migration architecture of IR5 and characterization parameters of IR6, it can be seen that the value of S is 2.01, C is 0.0008, reflecting a greater degree of bending;  $\Delta\theta$  is 19° and  $\Delta\theta'$  is -19°, indicating that the curvature apex is closer to the upstream bend inflection with the tendency of counter-current rotation.  $K_M$  is 1.20, indicating that the river bend is in the expansion period with a greater degree. Comprehensively, the meander 38 shows the architecture of URES.

### Downstream Rotation Expansion Structure

The meandering loop continuously erodes the outer banks with curvature apex being closer to the downstream bend inflection, showing a tendency of along-current rotation,  $K_M$  is greater

than 1 and  $\Delta\theta$  is negative, this is the Downstream Rotation Expansion Structure (DRES). As shown in Figure 3 IR7-IR9, IR7 shows that from years 1984 to 2013, the migration process is slow, and it is shown that value of S is 1.57 and C is 0.0005 by the planform migration architecture of IR8 and characterization parameters of IR9, reflecting a greater degree of bending;  $\Delta\theta$  is -37° and  $\Delta\theta'$  is 37°, indicating that the curvature apex is closer to the downstream bend inflection with the tendency of along-current rotation.  $K_M$  1.78, indicating that the river is in the expansion period with a greater degree. Comprehensively, the meander 18 shows the architecture of DRES.

### Constriction Structure

The Constriction Structure (CS) is characteristic as the constant erosion near the two points of bend inflection which tend to cut off along with the direction of meandering belt axis. The value of  $K_M$  is usually less than 1. According to the swing difference of meandering loops and point bar and the value of  $\Delta\theta$  and  $\Delta\theta'$ , it can also be specifically subdivided into 3 parts (Figure 4): Symmetrical Constriction Structure, Upstream Rotation Constriction Structure, and Downstream Rotation Constriction Structure.

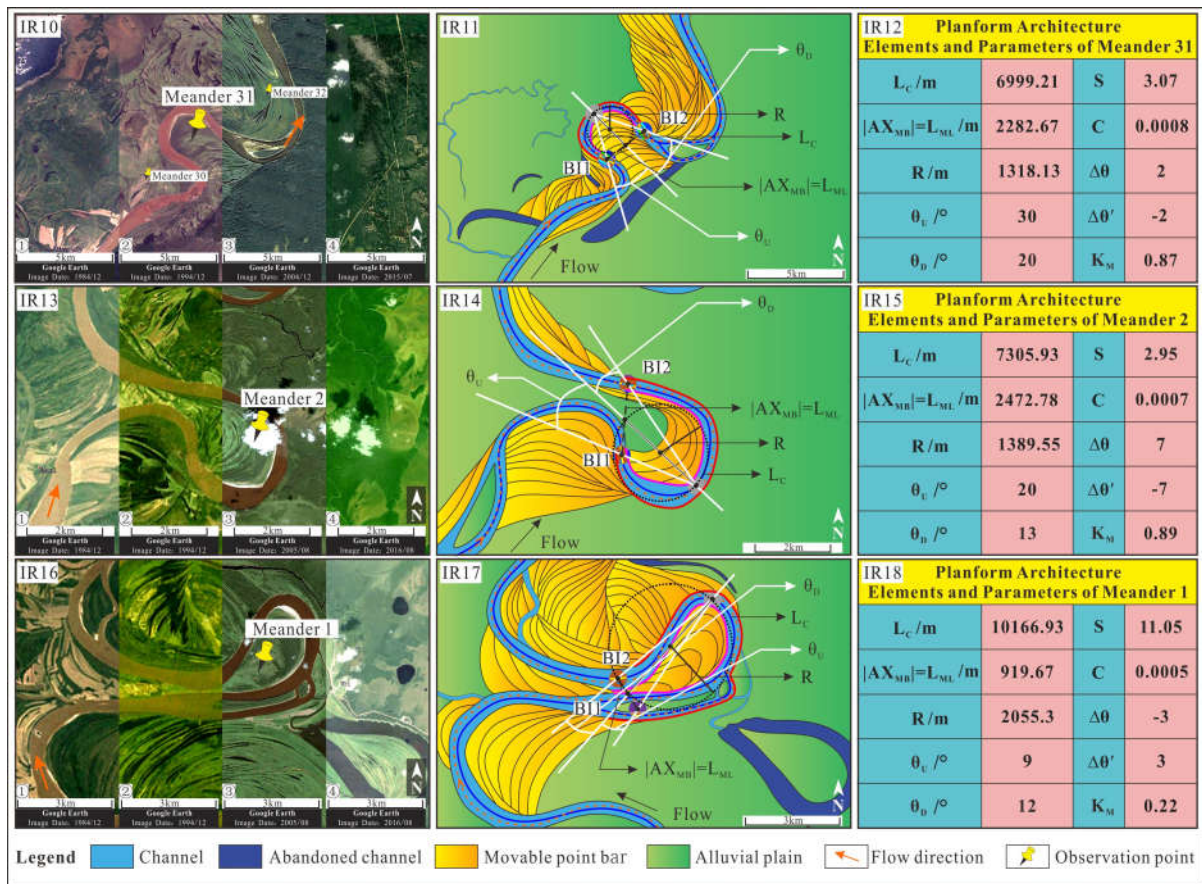


**Figure 4. Planform migration architecture of the Constriction Structure of the Irtysh River: IR10-IR12 is the performance of Symmetrical Constriction Structure in meander 31, while IR10 shows the satellite images taken in the last 30 years and coordinates are 60°14'N, 69°48'E; IR11 shows the planform migration architecture in details; and IR12 shows the statistical data of planform migration architecture elements and parameters of meander 31. IR13-IR15 is the performance of Upstream Rotation Constriction Structure in meander 2, while IR13 shows the satellite images taken in the last 30 years and coordinates are 58°56'N, 68°50'E; IR14 shows the planform migration architecture in details, and IR15 shows the statistical data of planform migration architecture elements and parameters of meander 2. IR16-IR18 is the performance of Downstream Rotation Constriction Structure in meander 1, while IR16 shows the satellite images taken in the last 30 years and coordinates are 58°52'N, 68°47'E; IR17 shows the planform migration architecture in details, and IR18 shows the statistical data of planform migration architecture elements and parameters of meander 1. Images and coordinates information come from Google Earth and ACME Mapper**

### Symmetrical Constriction Structure

The process of outward expansion of the meandering loop slows down and the symmetry is maintained, and the trend of cut-off is starting gradually near the bend inflections.  $K_M$  is less than 1 and  $\Delta\theta$  is close to 0°, this is the Symmetrical Constriction Structure (SCS). As shown in Figure 4 IR10-IR12, IR10 shows the satellite images of meander 31 from years 1984 to 2015, the migration of riverbed 31 is relatively slow. Through the planform migration architecture of IR11 and characterization parameters of IR12, it can be seen that the value of S is 3.07, C is 0.0008, reflecting the higher bending degree;  $\Delta\theta$  is 2° and  $\Delta\theta'$  is -2°, indicating that the symmetry of the bend is relatively better with a slight trend of counter-current rotation.  $K_M$  is 0.87, revealing that the river is in the constriction period, and the degree of constriction is small. Comprehensively, the meander 31 shows the architecture of SCS.

### Upstream Rotation Constriction Structure

The process of outward expansion of the meandering loop slows down with curvature apex being closer to the upstream bend inflection, showing a tendency of counter-current

rotation, and the trend of cut-off is starting gradually near the bend inflections.  $K_M$  is less than 1 and  $\Delta\theta$  is positive, this is the Upstream Rotation Constriction Structure (URCS). As shown in Figure 4 IR13-IR15, IR13 shows that from years 1984 to 2016, the migration of the meander 2 in the Irtysh River is slow. Through the planform migration architecture of IR14 and characterization parameters of IR15, it can be seen that the value of S is 2.95, C is 0.0007, reflecting a greater degree of bending;  $\Delta\theta$  is 7° and  $\Delta\theta'$  is -7°, indicating that the curvature apex is closer to the upstream bend inflection with the tendency of counter-current rotation.  $K_M$  is 0.89, indicating that the meander is in the constriction period with a greater degree. Comprehensively, the meander 2 shows the architecture of URCS.

### Downstream Rotation Constriction Structure

The process of outward expansion of the meandering loop slows down with curvature apex being closer to the downstream bend inflection, showing a tendency of along-current rotation, and the trend of cut-off is starting gradually near the bend inflections.  $K_M$  is less than 1 and  $\Delta\theta$  is negative, this is the Downstream Rotation Constriction Structure (DRCS). As shown in Figure 4 IR16-IR18, IR16 shows that

from years 1984 to 2016, the migration process of the meander 1 is not clear, and it is shown that value of  $S$  is 11.05 and  $C$  is 0.0005 by the planform migration architecture of IR17 and characterization parameters of IR18, reflecting a greater degree of bending;  $\Delta\theta$  is  $-3^\circ$  and  $\Delta\theta'$  is  $3^\circ$ , indicating that the curvature apex is closer to the downstream bend inflection with the tendency of along-current rotation.  $K_M$  0.22, indicating that the river is in the constriction period with a greater degree. Comprehensively, the meander 1 shows the architecture of DRCS.

and  $\Delta\theta'$  are basically maintained at  $0^\circ$ .  $K_M$  is always greater than 1, as shown in Figure 5 SEM, this is the meandering model of Symmetrical Expansion Migration (SEM). The meander 11 in IR1 (Figure 3) reveals this model.

**Upstream Rotation Expansion Migration**

The meandering channel continuously migrate laterally and the curvature apex is approximately shifting with curvilinear movement towards the upstream.

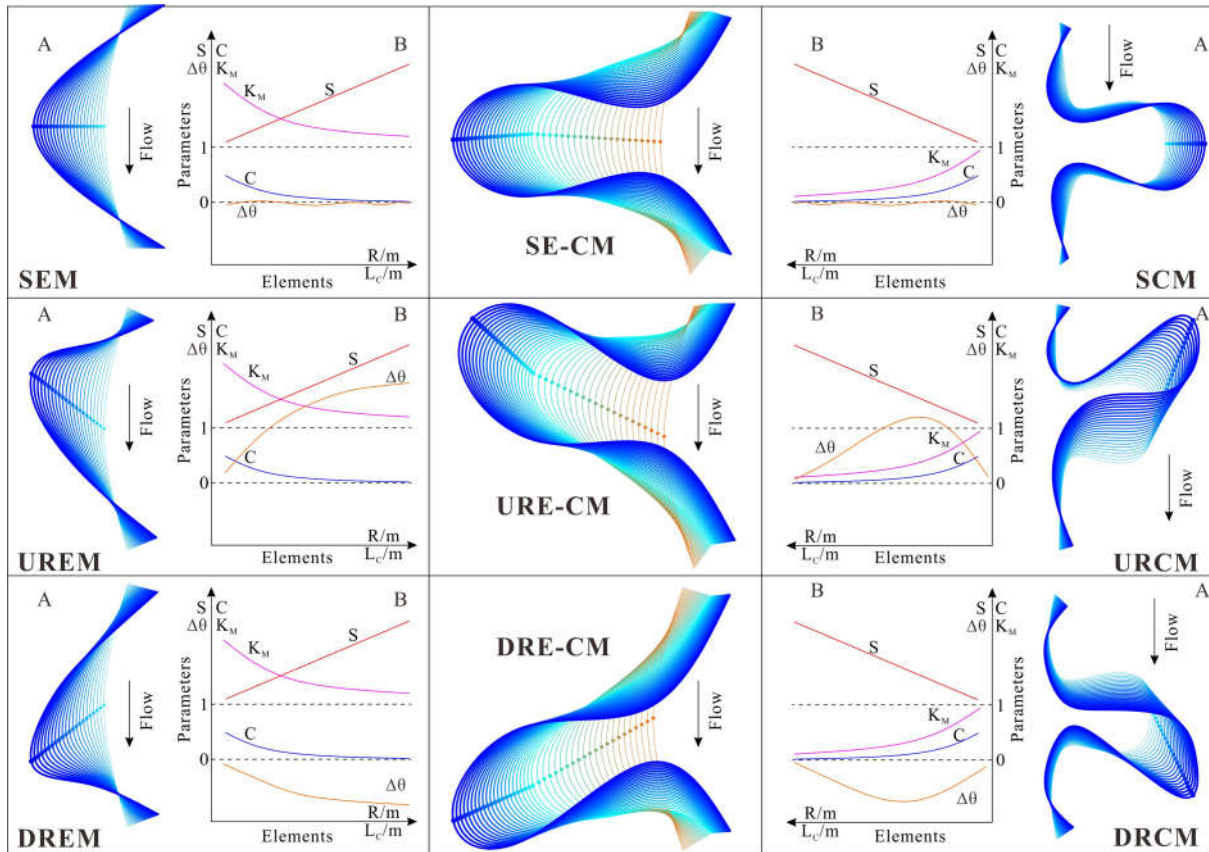


**Figure 5. Planform migration model of the meandering channel under the ideal condition: A is the simplified schematic diagram of the process of channel migration, and B is the simplified relation between the values of characterization parameter and structural elements**

**Channel migration model of meandering rivers**

Through the characterization and analysis of planform migration architecture, we can obtain the migration model of meandering channel in this paper. As the centerline could be approximated instead of the river channel, hence here the centerline replaces the river to simplify the migration process of the meandering channel and the migration model is established. Combining the characteristics of the above structural elements, the following ideal models for meandering rivers are established as 6 conventional models and 3 basic composite models (Figure 5).

**Expansion Migration Model**

**Symmetrical Expansion Migration**

The meandering channel continuously migrate laterally and the curvature apex is approximately shifting with linear movement. The value of  $L_C$ ,  $S$ , and  $R$  increases gradually, while the  $|AX_{MB}|$  and  $L_{ML}$  remain relatively stable with slow decrease,  $C$  decreases gradually;  $\theta_U$  and  $\theta_D$  remain constant,  $\Delta\theta$

The value of  $L_C$ ,  $S$ ,  $R$ , and  $\theta_U$  increases gradually, while the  $|AX_{MB}|$  and  $L_{ML}$  remain relatively stable with slow decrease,  $C$  and  $\theta_D$  decreases gradually;  $\Delta\theta$  is positive and increases gradually while  $\Delta\theta'$  is negative and decreases gradually.  $K_M$  is always greater than 1, as shown in Figure 5 UREM, this is the meandering model of Upstream Rotation Expansion Migration (UREM). The meander 38 in IR4 (Figure 3) reveals this model.

**Downstream Rotation Expansion Migration**

The meandering channel continuously migrate laterally and the curvature apex is approximately shifting with curvilinear movement towards the downstream. The value of  $L_C$ ,  $S$ ,  $R$ , and  $\theta_D$  increases gradually, while the  $|AX_{MB}|$  and  $L_{ML}$  remain relatively stable with slow decrease,  $C$  and  $\theta_U$  decreases gradually;  $\Delta\theta$  is negative and decrease gradually while  $\Delta\theta'$  is positive and increases gradually.  $K_M$  is always greater than 1, as shown in Figure 5 DREM, this is the meandering model of Downstream Rotation Expansion Migration (DREM). The meander 18 in IR7 (Figure 3) reveals this model.

## Constriction Migration Model

### Symmetrical Expansion Migration

The process of migrating laterally of the meandering channel slows down with the tendency of cut-off is beginning tardily near the bend inflections, and the curvature apex is approximately shifting with linear movement. The value of  $L_C$ ,  $S$ , and  $R$  increases slowly, while the value of  $|AX_{MB}|$ ,  $L_{ML}$ , and  $C$  relatively decrease.  $\Delta\theta_U$  and  $\Delta\theta_D$  remain constant,  $\Delta\theta$  and  $\Delta\theta'$  are basically maintained at  $0^\circ$ .  $K_M$  is always less than 1, as shown in Figure 5 SCM, this is the meandering model of Symmetrical Constriction Migration (SCM). The meander 31 in IR10 (Figure 4) reveals this model.

### Upstream Rotation Constriction Migration

The process of migrating laterally of the meandering channel slows down with the tendency of cut-off is beginning tardily near the bend inflections, and the curvature apex is approximately shifting with curvilinear movement towards the upstream. The value of  $L_C$ ,  $S$ , and  $R$  increases gradually, while the value of  $|AX_{MB}|$ ,  $L_{ML}$ , and  $C$  relatively decrease.  $\theta_U$  varies with early increase and later decrease while  $\theta_D$  with early decrease and later increase and then decrease;  $\Delta\theta$  is positive while  $\Delta\theta'$  is negative and both close to  $0^\circ$ .  $K_M$  is always less than 1, as shown in Figure 5 URCM, this is the meandering model of Upstream Rotation Constriction Migration (URCM). The meander 2 in IR13 (Figure 4) reveals this model.

### Downstream Rotation Constriction Migration

The process of migrating laterally of the meandering channel slows down with the tendency of cut-off is beginning tardily near the bend inflections, and the curvature apex is approximately shifting with curvilinear movement towards the downstream. The value of  $L_C$ ,  $S$ , and  $R$  increases gradually, while the value of  $|AX_{MB}|$ ,  $L_{ML}$ , and  $C$  relatively decrease.  $\theta_U$  varies with early decrease and later increase and then decrease while  $\theta_D$  with early increase and later decrease;  $\Delta\theta$  is negative while  $\Delta\theta'$  is positive and both close to  $0^\circ$ .  $K_M$  is always less than 1, as shown in Figure 5 DRCM, this is the meandering model of Downstream Rotation Constriction Migration (DRCM). The meander 1 in IR16 (Figure 4) reveals this model.

### Composite Migration Model

The migration process of the meandering channel is accompanied by changes in the topography, hydrodynamic, sedimentary environment and so on. Therefore, in the nature channel, it is more inclined to see the complexes of the above 6 model. While the basic composite models are these three: Symmetrical Expansion - Constriction Migration (SE-CM), Upstream Rotation Expansion - Constraint Migration (URE-CM), Downstream Rotation Expansion - Constriction Migration (DRE-CM). Other more complex migration situations can be basically combined by these patterns.

## DISCUSSION AND CONCLUSION

The purpose of this paper is to make a detailed characterization for the planform migration architecture of

meandering rivers by making full use of modern satellite photographs and historical images, and then in-depth analysis and discussion of the migration laws. We put forward a set of new concrete and feasible characterization parameter for the structure of the meandering channel, and to extract the feasible forecasting model. The study shows that the planform migration process of the meandering channel can be divided into 6 conventional and 3 basic composite models. Through different combinations, it can be used to describe and show the migration structure of modern and ancient rivers. The detailed description of the typical meanders on the 12 section of the Irtysh River has also been reflected in the migration structure. However, this article also has some limitations, although the identify and research on the typical natural river of Irtysh, it is still only the tip of the iceberg to the complex numbers of rivers in the world. Therefore, the methods and models in the study are still needed to be further studied in the future.

## REFERENCES

- Blum, M., J. Martin, *et al.*, 2013. Paleovalley systems: Insights from Quaternary analogs and experiments. *Earth-Science Reviews* 116: 128-169.
- Brice, J. C. (1974). Evolution of meander loops. *Geological Society of America Bulletin* 85(4): 581-586.
- Debnath, J., N. D. Pan, *et al.*, 2017. Channel migration and its impact on land use/land cover using RS and GIS: A study on Khowai River of Tripura, North-East India. *The Egyptian Journal of Remote Sensing and Space Science*.
- Feng, Z. 2013. *Chinese sedimentology (Second Edition)*. Beijing, Petroleum Industry Press.
- Fryirs, K. A. 2017. River sensitivity: a lost foundation concept in fluvial geomorphology. *Earth Surface Processes and Landforms* 42(1): 55-70.
- Ghinassi, M., A. Ielpi, *et al.*, 2016. Downstream-migrating fluvial point bars in the rock record. *Sedimentary Geology* 334: 66-96.
- Ghinassi, M., W. Nemeč, *et al.*, 2014. Plan—form evolution of ancient meandering rivers reconstructed from longitudinal outcrop sections. *Sedimentology* 61(4): 952-977.
- Gilvear, D., S. Winterbottom, *et al.*, 2000. Character of channel planform change and meander development: Luangwa River, Zambia. *Earth Surface Processes and Landforms* 25(4): 421-436.
- He, Y. and W. Wang 2008. *Sedimentary rocks and sedimentary facies*. Beijing, Petroleum Industry Press.
- Hooke, J. 1980. Magnitude and distribution of rates of river bank erosion. *Earth Surface Processes and Landforms* 5(2): 143-157.
- Hooke, J. 1984. Changes in river meanders: a review of techniques and results of analyses. *Progress in Physical Geography* 8(4): 473-508.
- Hu, G., F. Chen, *et al.*, 2017. Subdividing and comparing method of the fluvial facies reservoirs based on the complex sandbody architectures. *Petroleum Geology & Oilfield Development in Daqing* 36(2): 12-18.
- Hu, G., T. Fan, *et al.*, 2017. From Reservoir Architecture to Seismic Architecture Facies: Characteristic Method of a High-Resolution Fluvial Facies Model. *Acta Geographica Sinica* 91(2): 465-478.
- Hu, H. 2016. Adjustment measures of remaining oil tapping based on sand body structure. *Lithologic Reservoirs* 28(4): 113-120.

- Ielpi, A. and M. Ghinassi 2014. Planform architecture, stratigraphic signature and morphodynamics of an exhumed Jurassic meander plain (Scalby Formation, Yorkshire, UK). *Sedimentology* 61(7): 1923-1960.
- Kasvi, E., L. Laamanen, *et al.*, 2017. Flow Patterns and Morphological Changes in a Sandy Meander Bend during a Flood—Spatially and Temporally Intensive ADCP Measurement Approach. *Water* 9(2): 106.
- Leopold, L. B. 1960. Flow resistance in sinuous or irregular channels, US Government Printing Office.
- Leopold, L. B. and M. G. Wolman, 1957. River channel patterns: braided, meandering, and straight, US Government Printing Office.
- Leopold, L. B. and T. Maddock, 1953. The hydraulic geometry of stream channels and some physiographic implications, US Government Printing Office.
- Lin, Z., J. Shan, *et al.*, 2017. Meticulous Depiction and Genetic Mechanism of Unconformity Belt Structure. *Earth Science Research* 6(2): 19.
- Miall, A. D. 1985. Architectural-element analysis: a new method of facies analysis applied to fluvial deposits. *Earth-Science Reviews* 22(4): 261-308.
- Miall, A. D. 2013. The geology of fluvial deposits: sedimentary facies, basin analysis, and petroleum geology, Springer.
- Miall, A. D. 2014. Fluvial depositional systems, Springer.
- Miall, A. D. 2016. Facies Models. *Stratigraphy: A Modern Synthesis*, Springer: 161-214.
- Mithun, D., D. Dabojani, *et al.*, 2012. Evaluation of meandering characteristics using RS & GIS of Manu River. *Journal of Water Resource and Protection* 2012.
- Mu, L. 2000. Stages and characteristic of reservoir description. *Acta Petrolei Sinica* 21(5): 103-108.
- Schuurman, F., M. G. Kleinhans, *et al.*, 2016. Network response to disturbances in large sand-bed braided rivers. *Earth Surface Dynamics* 4(1): 25-45.
- Shi, S., S. Hu, *et al.*, 2012. Building geological knowledge database based on Google Earth software. *Acta Sedimentologica Sinica* 30(5): 869-878.
- Sui, X. 2006. A study on internal architecture of channel sand in meandering river, Northeast Petroleum University.
- Williams, G. P. (1978). Bank-full discharge of rivers. *Water Resources Research* 14(6): 1141-1154.
- Willis, B. J. and H. Tang, 2010. Three-dimensional connectivity of point-bar deposits. *Journal of Sedimentary Research* 80(5): 440-454.
- Wolman, M. G. and J. P. Miller. 1960. Magnitude and frequency of forces in geomorphic processes. *The Journal of Geology* 68(1): 54-74.
- Wu, C., J. P. Bhattacharya, *et al.*, 2015. Paleohydrology and 3D facies architecture of ancient point bars, Ferron Sandstone, Notom Delta, south-central Utah, USA. *Journal of Sedimentary Research* 85(4): 399-418.
- Wu, C., M. S. Ullah, *et al.*, 2016. Formation of point bars through rising and falling flood stages: Evidence from bar morphology, sediment transport and bed shear stress. *Sedimentology* 63(6): 1458-1473.
- Wu, S. and Z. Wang, 1999. A new method of non-marine reservoir flow unit study. *Acta Sedimentologica Sinica* 17(2): 87-92.
- Xue, P. 1991. An introduction to reservoir models of point bar facies. Beijing, Petroleum Industry Press.
- Yin, T., C. Zhang, *et al.*, 2001. Remaining oil distribution prediction based on high-resolution sequence stratigraphy. *Petroleum Exploration and Development* 28(4): 79-82.
- Zhu, X. 2008. Sedimentary petrology. Beijing, Petroleum Industry Press.

\*\*\*\*\*